Research in Astron. Astrophys. **2011** Vol. **11** No. **12**, 1413–1428
http://www.raa-journal.org *http://www.iop.org/journals/raa*

***R**esearch in*
***A**stronomy and*
***A**strophysics*

The relationship between the radio core dominance parameter and the spectral index in different classes of extragalactic radio sources *

Jun-Hui Fan[1,2], Jiang-He Yang[1,3], Jing Pan[1,2] and Tong-Xu Hua[1,2]

[1] Center for Astrophysics, Guangzhou University, Guangzhou 510006, China;
jhfan_cn@yahoo.com.cn
[2] Astronomy Science and Technology Research Laboratory of Department of Education of Guangdong Province, Guangzhou 510006, China
[3] Department of Physics and Electronics Science, Hunan University of Arts and Science, Changde 415000, China

Received 2011 March 31; accepted 2011 July 6

Abstract Active galactic nuclei (AGNs) have two major classes, namely radio loud AGNs and radio quiet AGNs. A small subset of the radio-loud AGNs is called blazars, which display extreme observational properties, such as rapid variability, high luminosity, high and variable polarization, and superluminal motion. All of those observational properties are probably due to a relativistic beaming effect with the jet pointing close to the line of sight. Observations suggest that the orientation can be expressed by a core-dominance parameter, R. The R, to some extent, is associated with the beaming effect. Blazars are believed to be unified with Fanaroff & Riley type I/II (FRI/II) radio galaxies. In this work, we collected relevant observations from the literature for a sample of 1223 AGNs including 77 BL Lacertae objects, 495 quasars, 460 galaxies, 119 FRs and 72 unidentified sources, and calculated the core-dominance parameters and spectral indexes, discussed the relationship between the two parameters, and gave some discussions. Our analysis suggests that the core-dominance parameters in BL Lacertae objects are larger than those in quasars and galaxies, and the radio spectral indexes in BL Lacertae objects are lower than those in quasars and galaxies. We also found that the core-dominance parameter-spectral index correlation exists for a large sample presented in this work, which may come from a relativistic beaming effect.

Key words: galaxies: active — galaxies: general — galaxies: jets — quasars: general

1 INTRODUCTION

Active galactic nuclei (AGNs) are interesting extragalactic radio sources. Among AGNs, roughly 85% are radio-quiet AGNs and the remaining $\sim$ 15% of AGNs are radio-loud ones (Fan 2005). A small subset of the radio-loud AGNs, showing extreme observation properties, is called blazars. Blazars, a word which was coined by Ed Spiegel in 1978, consist of two subclasses, namely the

---

* Supported by the National Natural Science Foundation of China.

BL Lacertae (BL Lac) objects and the optically violent variable (OVV) quasars. There are also some objects showing the properties of both the BL Lac and the OVV classes, which are also called blazars. There are differences within blazars in terms of their emission-line properties, which means that blazars can be divided into two groups: BL Lacs and those which are similar to quasars, called highly polarized quasars (HPQs), or the OVV quasars or more generally flat spectrum radio quasars (FSRQs) (Maraschi & Rovetti 1994). BL Lac objects have a very weak emission line feature, or have no emission lines at all in some cases, while FSRQs have very strong emission lines. However, both subclasses are almost the same in the continuum emissions. It is interesting that most AGNs in the first catalog of the Fermi mission are blazars (Abdo et al. 2010). The similarity in continuum and the difference in emission lines between BL Lacs and FSRQs have attracted authors' interest (see Fan 2003, and references therein).

Blazars show extreme observation properties, such as high and variable luminosity, high and variable polarization, no emission line or emission lines which are very strong, superluminal motions in their radio components, and high gamma-ray emission. They have attracted a good deal of attention from astronomers worldwide, searching for their emission mechanism, central structure, and evolution among different types of subclasses of AGNs (see, e.g., Abdo et al. 2010; Aller et al. 2003; Andruchow et al. 2005; Cellone et al. 2007; Ciprini et al. 2007; Dai et al. 2009; Efimov et al. 2002; Fan 2003; Fan et al. 1997, 2008, 2009, 2010; Gupta et al. 2004; Kurtanidze et al. 2007; Romero et al. 2000, 2002; Wagner 1996; Wills et al. 1992; Wu et al. 2005; Xie et al. 2005; Zhang & Fan 2008). The extreme observation properties suggest that blazars have a strong beaming effect, namely blazars are associated with a relativistic beaming model. A beaming+black hole+accretion disk model is taken as a standard model for AGNs (Urry & Padovani 1995). It is believed that BL Lac objects are the Fanaroff & Riley type I (FRI), whose jet points toward the observer, namely FRIs are the parent population of BL Lac objects (see Browne 1989; Ulrich 1989). The parent population of FSRQs is Fanaroff & Riley type II (FRII) (see Padovani & Urry 1992; Xie et al. 1993).

In the relativistic beaming model, the emissions are assumed to be from two components, namely the beamed and the unbeamed ones. Then, the observed total emission, $S^{\rm ob}$, is the sum of the beamed, $S_{\rm C}^{\rm ob}$, and the unbeamed, $S_{\rm Ext}$, emissions, so $S^{\rm ob} = S_{\rm Ext} + S_{\rm C}^{\rm ob} = (1 + f\delta^p)S_{\rm Ext}$; here $f = S_{\rm C}^{\rm in}/S_{\rm Ext}$, $S_{\rm C}^{\rm in}$ is the de-beamed emission in the co-moving frame, δ is a beaming factor, $p = \alpha$ + 2 (for a continuous jet case) or $p = \alpha$ +3 (for a moving sphere jet case), and α is the spectral index ($S_\nu \propto \nu^{-\alpha}$). Scheuer & Readhead (1979) defined the ratio, R, of the two parts as the core-dominance parameter (also see Orr & Browne 1982). Some authors use the ratio of flux densities while some others use the ratio of luminosities to indicate the parameter. Namely, $R = S_C/S_{\rm Ext}$ (or $R = L_{\rm C}/L_{\rm Ext}$); here S_C (or $L_{\rm C}$) stands for core emission while $S_{\rm Ext}$ (or $L_{\rm Ext}$) for extended emission (see Fan & Zhang 2003 and reference therein).

In 1992, Wills et al. (1992) obtained a sample of radio sources with known optical polarization and core-dominance parameter and found the polarization to be associated with this parameter; the larger the core-dominance parameter, the higher the polarization. This association is revisited in our previous work (Fan 2002). Core-dominance parameters were also calculated for a larger sample of extragalactic radio sources, as described in our previous paper (Fan & Zhang 2003). We also investigated the difference in the core-dominance parameter between FSRQs and BL Lac objects, and found that the core-dominance parameter in BL Lac objects is higher than that in FSRQs, which was confirmed by Britzen et al. (2007). One reason for BL Lac objects to have higher R-values than flat-spectrum radio quasars is that they may have different parent populations.

Correlations between the core-dominance parameter and other observations and parameters are discussed in the literature. Punsly (1995) studied the extended luminosity of strong radio cores for a sample of 134 ultraluminous radio core quasars, and found that the extended luminosity is on the order of weak FRII luminosity for most studied objects. Murphy et al. (1993) investigated a complete sample of 89 powerful core-dominated radio sources with core flux density, $S_c^{\rm 5GHz} > 1$ Jy at 5 GHz. They found that BL Lac objects on average are not more-dominated than quasars, they are beamed cores of FRI radio galaxies, and that some BL Lac objects with high redshift have similar extended radio emissions of FRII radio galaxies. Hough & Readhead (1989) defined a complete sample of 28 double-lobed radio quasars to check for consistency with the beaming hypothesis in the central components. Hutchings et al. (1988), Neff et al. (1989) and Neff & Hutchings (1990) discussed a large sample of 250 core-dominated quasars, and found that the core dominance parameter increases with redshift. Qin et al. (1998) used different samples to investigate the correlation between the core-dominance parameter and the core-/extended-luminosity, and obtained different correlations. A clear anti-correlation between the core-dominance parameter and extended emission for one sample did not show up for another sample. A similar situation appeared in the correlation analysis of the core-dominance parameter and the core-emission. Liu & Zhang (2002) compiled a larger sample of 661 extragalactic radio sources to investigate the correlation between the 5 GHz core luminosity and the 1.4 GHz total luminosity. Fan & Zhang (2003) calculated core-dominance parameters for a sample of extragalactic radio sources and investigated the correlation between the luminosity and the core-dominance parameter, finding that core-emissions are correlated with the core-dominance parameter when the core-dominance parameters are small enough, and there is no such core relationship when the core-dominance parameter is large enough. For the extended emissions and core-dominance parameter, there is an anti-correlation when the core-dominance parameter is large enough.However there is no such correlation when the core-dominance parameter is small enough. That is why a different correlation between the core-dominance parameter and core-/extended-emission was obtained in the work by Qin et al. (1998) and references therein. In 2010, based on a paper by Kovalev et al. (2005), we adopted the total and the core flux densities and calculated the core-dominance parameter for a sample of blazars and investigated the correlation between the parameter and the spectral index, finding that there is an association between the core-dominance parameter and the spectral index (Fan et al. 2010). From the above work, we can see that the core-dominance parameter is associated with the beaming effect in AGNs.

In a two-component model, if the intrinsic flux of a jet, $S_{\rm C}^{\rm in}$, is assumed to be composed of a polarized part, $S_{\rm C}^{\rm p}$ and an unpolarized part, $S_{\rm C}^{\rm up}$, and the two parts are proportional to each other as $S_{\rm C}^{\rm p} = \eta S_{\rm C}^{\rm up}$, then the polarization can be expressed in the following form (see Fan et al. 1997, 2008),

$$P^{\rm ob} \sim \frac{R}{1+R}\frac{\eta}{1+\eta}. \tag{1}$$

If the emissions are from a synchrotron process, then we find that the polarization and the spectral index follow the relation

$$P(\%) \propto \frac{\alpha+1}{\alpha+(5/3)}. \tag{2}$$

The above relationships (1) and (2) suggest a correlation between the core-dominance parameter and the spectral index (Fan et al. 2010). In this work, we collected a larger sample of radio sources, calculated the core-dominance parameter and the spectral index, and revisited the correlation between them. The paper is arranged as follows: in Section 2 we give the compiled sample, display how we calculated the core-dominance parameter and the radio spectral index and present some results. In Section 3, we provide some discussions and a conclusion.

2 SAMPLE AND RESULTS

2.1 Sample and Calculations

To calculate the core-dominance parameter and discuss its properties, we compiled the relevant data from the literature. Generally, the observations are performed at different frequencies in different references. However, our investigation indicates that most of the radio data are at 5 GHz, therefore, we transformed the data, given in the literature at other frequencies (ν), to 5 GHz using the assumption $S_C^{5\rm GHz} = S_C^{\nu,\rm obs}$, $S_{\rm Ext}^{5\rm GHz} = S_{\rm Ext}^{\nu,\rm obs}(\frac{\nu}{5\rm GHz})^{\alpha_{\rm Ext}}$, then we K-corrected the emissions, and finally calculated the core-dominance parameter using $\log R = \log(S_C/S_{\rm Ext})(1+z)^{\alpha_{\rm C}-\alpha_{\rm Ext}}$. In our calculation, we adopted $\alpha_{\rm Ext}$ (or $\alpha_{\rm unb}$) = 0.75 and α_C (or $\alpha_{\rm j}$) = 0.0. Some data given in the literature are luminosities; if the luminosity is not at 5 GHz, we also transformed the luminosities to the 5 GHz frequency. Then we calculated the core-dominance parameter using $\log R = \log(L_{\rm C}/L_{\rm Ext})$. We also obtained the radio data (mainly at 1.4 and 5 GHz) from the literature (here mainly from NED), K-corrected them and calculated the spectral index, α ($S_\nu \propto \nu^{-\alpha}$). If a source had no redshift, then the averaged value of the corresponding group was adopted in our calculation. From the relevant literature, we got 1223 sources. We checked their identifications using the NED. When there is further classification for a galaxy, namely FRI and FRII, then we only use FRI or FRII to identify the source. If it is a Seyfert galaxy, then we use Seyfert. When we have not made the identification from NED, we use an unidentified source to indicate it. So, we have 77 BL Lac objects, 495 quasars, 460 galaxies, 119 FRs and 72 unidentified sources.

The data and their corresponding references are shown in Tables 1 and 2. In Table 1, Col. 1 gives the name of the source; Col. 2 classification (BL: BL Lac; I: FR type I radio galaxy; II: FR type II radio galaxy; G: galaxy; Q: quasar; S: Seyfert galaxy; U: unidentified source); Col. 3 redshift, z; Col. 4 radio spectral index, α ($S_\nu \propto \nu^{-\alpha}$); Col. 5 core-emission in $\rm mJy$; Col. 6 wavelength in $\rm cm$ for emission in Col. 5; Col. 7 Reference for Cols. 5 and 6; Col. 8 extended emission in $\rm mJy$; Col. 9 wavelength in $\rm cm$ for emission in Col. 5; Col. 10 Reference for Cols. 8 and 9; Col. 11 total emission in $\rm mJy$; Col. 12 wavelength in $\rm cm$ for emission in Col. 11; Col. 13 Reference for Cols. 11 and 12; Col. 14 the core-dominance parameter at 5 GHz $\log R$.

In Table 2, Col. 1 gives the name of the source; Col. 2 classification (the meaning of the letters are the same as in Table 1); Col. 3 redshift, z; Col. 4 radio spectral index, α ($S_\nu \propto \nu^{-\alpha}$); Col. 5 core-luminosity in $\rm WHz^{-1}$ at $6\rm cm$; Col. 6 extended-luminosity in $\rm WHz^{-1}$ at $6\rm cm$; Col. 7 total luminosity in $\rm WHz^{-1}$ at $6\rm cm$; Col. 8 reference for the luminosities in Col. 5, 6, and 7; Col. 9 core-dominance parameter at 5 GHz (6 cm) $\log R$. The spectral index, α ($S_\nu \propto \nu^{-\alpha}$), calculated from the relevant data, is listed in Table 3.

The references for Tables 1 and 2 are as follows: AU85: Antonucci & Ulvestad (1985); BCG98: Best et al. (1998); BEL99: Best et al. (1999); BIE81: Biermann et al. (1981); BLR97: Best et al. (1997); BM87: Browne & Murphy (1987); BP86: Browne & Perley (1986); BVL00: Barthel et al. (2000); CFG99: Cotton et al. (1999); FIK84: Feigelson et al. (1984); GCL91: Garrington et al. (1991); GH84: Gower & Hutchings (1984); HAP97: Hardcastle et al. (1997); HO81: Hintzen &

Table 1 Sample 1

Name	C	z	α	$S_{\rm c}$	λ	Ref.	$S_{\rm e}$	λ	Ref.	$S_{\rm t}$	λ	Ref.	$\log R$
0003+15	S	0.4509	0.66	135	6	MH78	223	6	MH78				−0.34
0003+380	S	0.2290	0.04	520	20	TVR96				601	20	TVR96	1.13
0003–003	Q	1.0370	0.74	1440	11	PW79	910	11	PW79				0.28
0007+106	S	0.0893	0.05	350	6	WB86	< 10	6	WB86				1.52
.....	...	...	...	...	...	...	...	...	...	...	...	...	...

Table 2 Sample 2

Name	C	z	α	$\log L_{\rm c}^{6\rm cm}$	$\log L_{\rm e}^{6\rm cm}$	$\log L_{\rm t}^{6\rm cm}$	Ref.	$\log R$
0007+171	Q	1.6010	−0.11	28.1	27.6		BM87	0.50
0015–229	G	2.0100	1.30	25.32		27.42	LZ02	−1.68
0019+230	G	0.1338	0.85	22.67		24.63	LZ02	−1.54
0031+060	G	0.1334	0.84	22.48		24.71	LZ02	−1.81
...	...	...	...	...	...	...	...	...

Owen (1981); HUO83: Hintzen et al. (1983); KAS98: Kapahi et al. (1998); KWR90: Kollgaard et al. (1990); LGS98: Ludke et al. (1998); LP91: Leahy & Perley (1991); LPP06: Landt et al. (2006); LZ02: Liu & Zhang (2002); MH78: Miley & Hartsuijker (1978); NED; NRH95: Neff et al. (1995); OO185: O'Dea & Owen (1985b); OO285: O'Dea & Owen (1985a); OPN78: Owen et al. (1978); P82: Perley (1982); PCR91: Parma et al. (1991); PFJ82: Perley et al. (1982); PGH93: Price et al. (1993); PS93: Perlman & Stocke (1993); PW79: Potash & Wardle (1979); RRM99: Riley et al. (1999); SSN87: Saikia et al. (1987a); SSC89: Saikia et al. (1989); SBR00: Schoenmakers et al. (2000); SHK98: Saikia et al. (1998); SJC90: Saikia et al. (1990); SSF91: Spencer et al. (1991); SWC87: Saikia et al. (1987b); TVR96: Taylor et al. (1996); UA86: Ulvestad & Antonucci (1986); WB86: Wills & Browne (1986); WHP88: Wrobel et al. (1988).

Table 3 Calculation of the Spectral Index

Name	C	$S_{\nu 1}$/Jy	ν_1/GHz	S_{ν_2}/Jy	$\nu 2$/GHz	$\alpha_{\nu 1}^{\nu 2}$	Ref
0003+15	4C+15.01	0.34	5	0.788	1.4	0.66	NED
0003+380	B3	0.547	4.85	0.573	1.4	0.04	NED
0003−003	3C2	1.41	5	3.61	1.4	0.74	NED
0007+106		0.28	5	0.3	1.4	0.05	NED
0007+124	4C12.03	0.533	4.85	1.007	1.4	0.51	NED
0007+171	4C17.04	0.943	4.85	0.825	1.4	−0.11	NED
.....	...	...	...	...	...	...	...

2.2 Results

From Tables 1 and 2, we can see, for the 1223 sources in the whole sample, that the core-dominance parameters are in the range of $\log R = -4.16$ for 1627+444 to $\log R = 3.44$ for 0256−005 with an average value of $\langle \log R \rangle = -0.35 \pm 1.24$; the radio spectral index is in the range $\alpha_{\rm t} = -0.83$ for 2134+004 to $\alpha_{\rm t} = 2.12$ for 1201+205 with an average value of $\langle \alpha_{\rm t} \rangle = 0.51 \pm 0.47$.

If we consider the subclasses separately, then for 77 BL Lac objects, we have $\log R = -0.68$ for 0837−12 to $\log R = 3.40$ for 0851+202 with an average value of $\langle \log R \rangle = 0.87 \pm 0.99$; the radio spectral index is in the range $\alpha_{\rm t} = -0.63$ for 0954+65 to $\alpha_{\rm t} = 0.91$ for 1620+103 with an average value of $\langle \alpha_{\rm t} \rangle = 0.16 \pm 0.34$.

For 495 quasars, we have $\log R = -2.85$ for 1318+113 to $\log R = 3.44$ for 0256−005 with an average value of $\langle \log R \rangle = 0.13 \pm 0.97$; the radio spectral index is in the range $\alpha_{\rm t} = -0.83$ for 2134+004 to $\alpha_{\rm t} = 1.37$ for 0730+257 with an average value of $\langle \alpha_{\rm t} \rangle = 0.36 \pm 0.47$.

For 460 galaxies and Seyfert galaxies, we have $\log R = -3.26$ for 1017+37 to $\log R = 2.10$ for 0953+254 with an average value of $\langle \log R \rangle = -0.72 \pm 1.06$; the radio spectral index is in the range $\alpha_{\rm t} = -0.77$ for 0923+392 to $\alpha_{\rm t} = 2.12$ for 1201+205 with an average value of $\langle \alpha_{\rm t} \rangle = 0.65 \pm 0.41$.

When we consider galaxies and Seyfert galaxies separately, then for 280 galaxies, we have $\log R = -3.26$ for 1017+37 to $\log R = 2.07$ for 0700+470 with an average value of $\langle \log R \rangle = -0.93 \pm 0.98$; the radio spectral index is in the range $\alpha_{\rm t} = -0.74$ for 1452−517 to $\alpha_{\rm t} = 2.12$ for 1201+205 with an average value of $\langle \alpha_{\rm t} \rangle = 0.73 \pm 0.36$; for 180 Seyfert galaxies, we have $\log R = -3.20$ for 1957+405 to $\log R = 2.10$ for 0953+254 with an average value of $\langle \log R \rangle = -0.39 \pm 1.11$; the radio spectral index is in the range $\alpha_{\rm t} = -0.77$ for 0923+392 to $\alpha_{\rm t} = 1.62$ for 1957+405 with an average value of $\langle \alpha_{\rm t} \rangle = 0.53 \pm 0.44$.

For 119 FR galaxies, we have $\log R = -4.16$ for 1627+444 to $\log R = 0.11$ for 1637+826 with an average value of $\langle \log R \rangle = -1.99 \pm 0.92$; the radio spectral index is in the range $\alpha_{\rm t} = 0.49$ for 1615+351 to $\alpha_{\rm t} = 1.60$ for 1626+396 with an average value of $\langle \alpha_{\rm t} \rangle = 0.94 \pm 0.20$.

For 72 unidentified sources, we have $\langle \log R \rangle = 0.10 \pm 1.19$ and $\langle \alpha_{\rm t} \rangle = 0.30 \pm 0.52$.

All those data are listed in Table 4, in which Col. 1 gives the subclass name of the sample, Col. 2 the averaged value of $\log R$, $\langle \log R \rangle$, Col. 3 the averaged value of α, $\langle \alpha \rangle$, and Col. 4 the number of

Table 4 Averaged Values

Sample	$\langle \log R \rangle$	$\langle \alpha \rangle$	N
Total	-0.351	0.509	1223
BL	0.866	0.161	77
FRI/II	-1.987	0.938	119
FRI	-1.411	0.802	18
FRII	-2.089	0.963	101
Gal/Sey	-0.717	0.648	460
Gal	-0.928	0.733	280
Seyf	-0.389	0.533	180
QSO	0.129	0.356	495
UID	0.095	0.297	72

the subclass. From Table 4, we have that the distributions of $\log R$'s and α's in different subclasses are different with $\log R|_{\rm BL\,Lac} > \log R|_{\rm QSOs} > \log R|_{\rm gal/Sey} > \log R|_{\rm FRI/II}$, and $\alpha|_{\rm BL\,Lac} < \alpha|_{\rm QSO} < \alpha|_{\rm Gal/Sey} < \alpha|_{\rm FRI/II}$ on average.

2.3 Core-Dominance Parameter and Spectral Index

From the core-dominance parameters and spectral indexes listed in Tables 1 and 2, we can investigate the differences between different subclasses. Here, we considered BL Lacs, quasars, FRI/FRII cases, and galaxies/Seyfert galaxies.

For BL Lacs and quasars, their distributions of $\log R$'s are shown in Figure 1(a). When a K-S test is applied to the data, the cumulative result is shown in Figure 1(b), from which we have $d_{\rm max} = 0.27$ at $\log R = 0.51$ and the probability for the two distributions to be from the same parent distribution is $p = 8.14 \times 10^{-5}$. The distributions of spectral indexes are shown in Figure 2(a). When a K-S test is applied to the data, the cumulative result is shown in Figure 2(b), from which we have $d_{\rm max} = 0.28$ at $\alpha = 0.47$ and the probability for the two distributions to be from the same parent distribution is $p = 3.80 \times 10^{-5}$.

For BL Lacs and galaxies/Seyfert galaxies, their distributions of $\log R$'s are shown in Figure 1(a), and the cumulative result is shown in Figure 1(b), from which we have $d_{\rm max} = 0.60$ at $\log R = -0.18$ and the probability for the two distributions to be from the same parent distribution is $p = 4.47 \times 10^{-22}$. The distributions of spectral indexes are shown in Figure 2(a), while the cumulative result is shown in Figure 2(b). We have $d_{\rm max} = 0.62$ at $\alpha = 0.49$ and the probability for the two distributions to be from the same parent distribution is $p = 4.6 \times 10^{-22}$.

For BL Lacs and FRI galaxies, their distributions of $\log R$'s are shown in Figure 1(a), and the cumulative result is shown in Figure 1(b). We have $d_{\rm max} = 0.89$ at $\log R = -0.68$ and the probability for the two distributions to be from the same parent distribution is $p = 3.11 \times 10^{-11}$. The distributions of spectral indexes and the cumulative result are shown in Figure 2(a) and Figure 2(b) respectively, from which we have $d_{\rm max} = 0.84$ at $\alpha = 0.49$ and the probability for the two distributions to be from the same parent distribution is $p = 4.96 \times 10^{-10}$.

For quasars and galaxies/Seyfert galaxies, their distributions of $\log R$'s and cumulative result are shown in Figure 1(a) and Figure 1(b) respectively, from which, we have $d_{\rm max} = 0.39$ at $\log R = -0.29$ and the probability for the two distributions to be from the same parent distribution is $p = 4.61 \times 10^{-32}$. Also, the distributions of spectral indexes and their cumulative result are shown in Figure 2(a) and Figure 2(b). We have $d_{\rm max} = 0.35$ at $\alpha = 0.47$ and the probability for the two distributions to be from the same parent distribution is $p = 4.95 \times 10^{-25}$. All the results are listed in Tables 5 and 6 for the core-dominance parameter and spectral indexes respectively.

When the spectral indexes in Tables 1 and 2 are plotted against the core dominance parameters, we can see their dependence as shown in Figure 3, where the open circles ($\circ$) stand for BL Lac, $\triangle$ for FRI and FRII, $\diamond$ for quasars, $\bigtriangledown$ for galaxies, $\triangleleft$ for Seyfert galaxies and $\triangleright$ for unidentified sources.

Table 5 Statistical Results for Core-dominance Parameter

Samp: I-II	$N_{\rm I}$	$N_{\rm II}$	$\log R$	$d_{\max}$	p
BL-Q	77	495	0.51	0.27	8.14×10^{-5}
BL-FRI	77	18	−0.68	0.89	3.11×10^{-11}
BL-GS	77	460	−0.18	0.6	4.47×10^{-22}
FRII-Q	101	495	−0.76	0.75	4.58×10^{-42}
Q-GS	495	460	−0.29	0.39	4.61×10^{-32}

Table 6 Statistical Results for Spectral Index

Samp: I-II	$N_{\rm I}$	$N_{\rm II}$	α	$d_{\max}$	p
BL-Q	75	486	0.47	0.28	3.80×10^{-5}
BL-FRI	75	18	0.49	0.84	4.96×10^{-10}
BL-GS	75	415	0.49	0.62	4.60×10^{-22}
FRII-Q	101	486	0.73	0.64	3.92×10^{-31}
Q-GS	486	415	0.47	0.35	4.95×10^{-25}

2.4 Correlation between Extended Luminosity and the Core-dominance Parameter

In the two-component beaming model, the core emissions are beamed while the extended emissions are unbeamed. The core-dominance parameter is an indication of the orientation; it can also be taken as an indication of a beaming effect. Here, we investigate the relationship between the beaming effect and the unbeamed emissions. To do so, we used the extended luminosity at 5 GHz. Here we firstly K-corrected the flux density, and then calculated luminosity, $L_\nu = 4\pi d^2 S_\nu$, where d is the luminosity distance obtained from the Λ-CDM model (Pedro & Priyamvada 2007) with $\Omega_\Lambda \simeq 0.7$, $\Omega_M \simeq 0.3$, $\Omega_K \simeq 0.0$ and $H_0 \simeq 75\,{\rm km\,s^{-1}\,Mpc^{-1}}$. For the luminosities presented in the literature that are not at 5 GHz, we transformed the luminosity into those at 5 GHz. In Figure 4, we show the plot of the extended luminosity against the core-dominance parameter for the whole sample.

3 DISCUSSION

A small number of AGNs show extreme observational properties, which are associated with a relativistic beaming effect, and the relativistic beaming boosting factor was estimated by using different methods (Ghisellini et al. 1993; Readhead 1994; Lähteenmäki & Valtaoja 1999; Xie et al. 2002, 2005; Fan et al. 1999, 2009). The core-dominance parameter, R, of an AGN was used as an orientation indicator of the jet. It is expressed as $R(\theta) = f((\Gamma(1-\beta\cos\theta))^{-p} + (\Gamma(1+\beta\cos\theta))^{-p})$ (see Urry & Padovani 1995), and can be expressed in the form $R \propto f\delta^p$ when the viewing angle θ is very small (Ghisellini et al. 1993). It correlates with the polarization (Wills et al. 1992; Fan et al. 2006, 2008). In AGNs, the radio emissions are known from a synchrotron process, which follows a correlation between radio polarization and radio spectral index. Therefore, one can expect a correlation between the spectral index and core-dominance parameter. In our previous work, a relationship was derived (Fan et al. 2010), namely,

$$\alpha_{\rm t} = \frac{R}{1+R}\alpha_{\rm C} + \frac{1}{1+R}\alpha_{\rm Ext}. \tag{3}$$

From the relation (3), given $\alpha_{\rm C}$ and $\alpha_{\rm Ext}$, the dependence of the radio spectral index, $\alpha_{\rm t}$, on the core-dominance parameter, R, can be obtained. In this paper, we compiled 1223 objects with the relevant data to calculate the core-dominance parameters. The sample is not complete, but it is big enough for statistical analysis. When the spectral indexes and the core dominance parameters in Tables 1 and 2 are plotted in Figure 3, we can see a clear trend for the spectral index $\alpha_{\rm t}$ to be associated with the core dominance parameter.

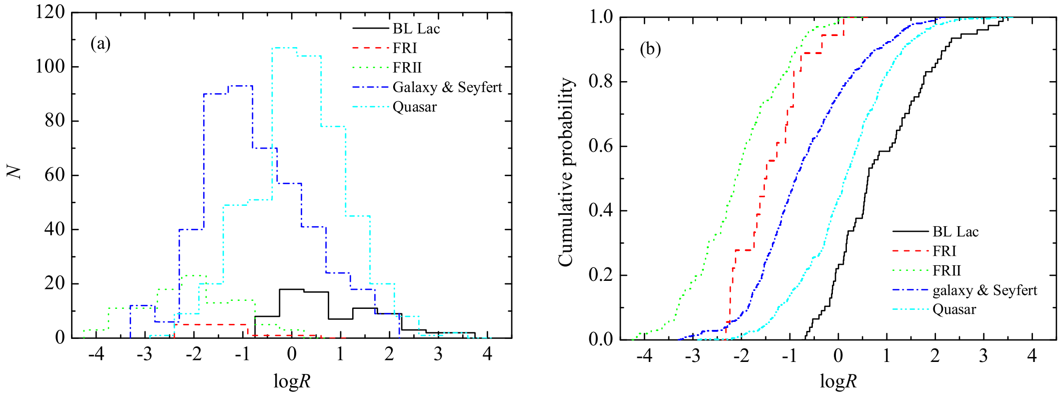

Fig. 1 Distribution of core-dominance parameter, $\log R$ (a) and the cumulative probability (b) for the whole sample. In this plot, solid line stands for BL Lac, broken line for FRI, dotted line for FRII, broken-dotted line for Galaxies/Seyfert galaxies and broken-dot-dotted line for quasars.

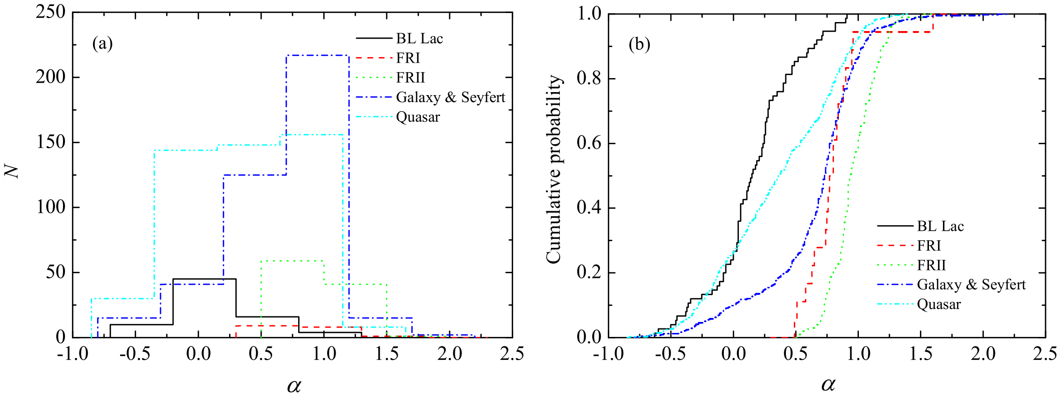

Fig. 2 Distribution of spectral index, $\alpha_{\rm t}$ (a) and the cumulative probability (b) for the whole sample. In this plot, solid line stands for BL Lac, broken line for FRI, dotted line for FRII, broken-dotted line for Galaxies/Seyfert galaxies and broken-dot-dotted line for quasars.

Figure 3 also suggests that we cannot use one curve to fit all of the points. The reason is that the spectral indexes, $\alpha_{\rm C}$ and $\alpha_{\rm Ext}$, are different for different sources. Besides, there is also a possibility that the flux densities used to calculate the spectral index and those used to calculate core dominance are not simultaneous, which results in the points scattering. If all of the sources follow relation (3), then we can estimate the spectral indexes, $\alpha_{\rm C}$ and $\alpha_{\rm Ext}$, for the whole sample by minimizing $\sum[\alpha-\alpha_{\rm C}R/(1+R)+\alpha_{\rm Ext}/(1+R)]^2$. When we adopted this across the whole sample, $\alpha_{\rm C}=-0.07$ and $\alpha_{\rm Ext}$ = 0.92 were obtained. The fitting result is shown in the curve fit in Figure 3. The fitting results are consistent with the general consideration taking $\alpha_{\rm C}$ = 0.0 and $\alpha_{\rm Ext}$ = 1.0.

When we considered the subclasses separately, we can obtain a plot of the spectral index against the core-dominance parameter as shown in Figure 5 for BL Lac objects. Their spectral index for emissions in the jet is in the range of $\alpha_{\rm C}=-0.65$ to 0.5, and their spectral index from the unbeamed emissions (or the extended emissions) is in the range of $\alpha_{\rm Ext}$ = 0.0 to 1.4. The fitting result gives $\alpha_{\rm C}=-0.01$ and $\alpha_{\rm Ext}$ = 0.65. In Figure 6 for quasars, their spectral index for emissions in the jet is in the range $\alpha_{\rm C}=-0.70$ to 0.5, and their spectral index from the unbeamed emissions (or the

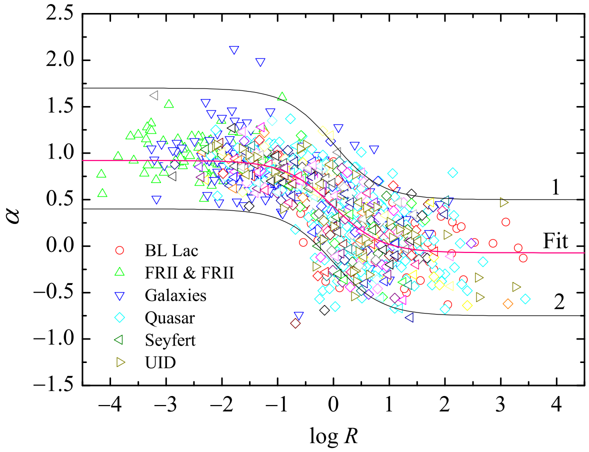

Fig. 3 Plot of the radio spectral index, $\alpha_{\rm t}$, against the core-dominance parameter, $\log R$, for the whole sample. Here ○ stands for BL Lac, △ for FRI and FRII, ◇ for quasars, ▽ for Galaxies, ◁ for Seyfert galaxies and ▷ for unidentified sources. Curve 1 corresponds to $\alpha_{\rm C}$ (or $\alpha_{\rm j}$) = 0.5 and $\alpha_{\rm Ext}$ (or $\alpha_{\rm unb}$) = 1.70, curve 2 corresponds to $\alpha_{\rm C}$ = –0.75 and $\alpha_{\rm Ext} = 0.4$ and the fitting curve corresponds to $\alpha_{\rm C}$=–0.07 and $\alpha_{\rm Ext} = 0.92$.

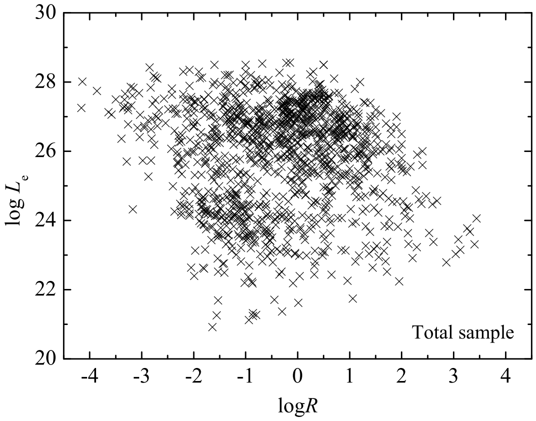

Fig. 4 Plot of the extended luminosity against the core-dominance parameter for the whole sample.

extended emissions) is in the range $\alpha_{\rm Ext}$ = 0.5 to 1.5. The fitting result gives $\alpha_{\rm C} = -0.09$ and $\alpha_{\rm Ext}$ = 0.89. In Figure 7 for galaxies and Seyfert galaxies, their spectral index for emissions in the jet is in the range $\alpha_{\rm C} = -0.75$ to 0.5, and their spectral index from the unbeamed emissions (or the extended emissions) is in the range $\alpha_{\rm Ext}$ = 0.5 to 1.6. The fitting result gives $\alpha_{\rm C} = -0.01$ and $\alpha_{\rm Ext}$ = 0.91. In Figure 8 for FRI/II galaxies, their spectral index for emissions from the jet is in the range $\alpha_{\rm C}$ = 0.34 to 0.4, and their spectral index from the unbeamed emissions (or the extended emissions) is in the range $\alpha_{\rm Ext}$ = 0.5 to 1.4. The fitting result gives $\alpha_{\rm C}$ = 0.34 and $\alpha_{\rm Ext}$ = 0.97.

It seems that the tendency for the spectral index to depend on the core-dominance parameter is probably from the relativistic beaming effect. From the averaged values of different subclasses of AGNs, we have a continuous trend in $\log R$ with $\log R|_{\rm BL} > \log R|_{\rm QSO} > \log R|_{\rm Gal} > \log R|_{\rm FRI/II}$, and in α with $\alpha|_{\rm BL} < \alpha|_{\rm QSO} < \alpha|_{\rm Gal} < \alpha|_{\rm FRI/II}$.

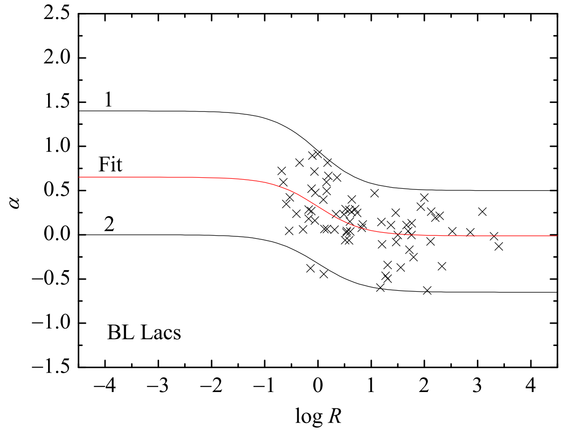

Fig. 5 Plot of the radio spectral index, $\alpha_{\rm t}$, against the core-dominance parameter for BL Lac objects. Curve 1 corresponds to $\alpha_{\rm C}$ (or $\alpha_{\rm j}$) = 0.5 and $\alpha_{\rm Ext}$ (or $\alpha_{\rm unb}$) = 1.40, curve 2 corresponds to $\alpha_{\rm C} = -0.65$ and $\alpha_{\rm Ext} = 0.0$, and the fitting curve corresponds to $\alpha_{\rm C} = -0.01$ and $\alpha_{\rm Ext} = 0.65$.

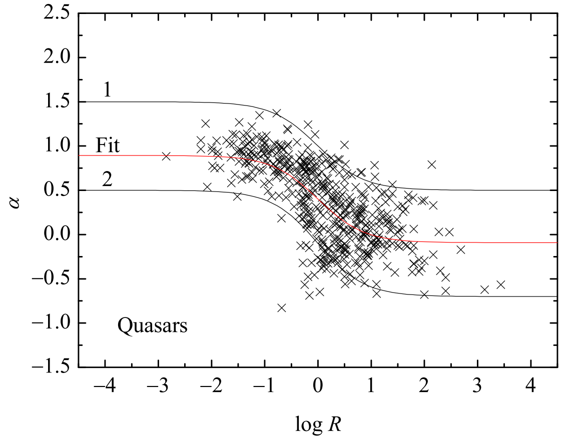

Fig. 6 Plot of the radio spectral index, $\alpha_{\rm t}$, against the core-dominance parameter for quasars. Curve 1 corresponds to $\alpha_{\rm C}$ (or $\alpha_{\rm j}$) = 0.5 and $\alpha_{\rm Ext}$ (or $\alpha_{\rm unb}$) = 1.50, curve 2 corresponds to $\alpha_{\rm C}$ = –0.7 and $\alpha_{\rm Ext} = 0.5$, and the fitting curve corresponds to $\alpha_{\rm C}$= –0.09 and $\alpha_{\rm Ext} = 0.89$.

In the extended luminosity and core-dominance parameter diagram (Fig. 4), we can see that there is a trend for the extended luminosity to be anti-correlated with the core-dominance parameter. In a two component model, $R = L_{\rm C}/L_{\rm Ext}$, which can be expressed in the form

$$1 + R = \frac{L_{\rm C} + L_{\rm Ext}}{L_{\rm Ext}} = \frac{L_{\rm T}}{L_{\rm Ext}}.$$

If $L_{\rm T} = L_{\rm C} + L_{\rm Ext}$ is a constant, then $R + 1$ is anti-correlated to $L_{\rm Ext}$ when R is much larger than unity, and there is no correlation between R and $L_{\rm Ext}$ when R is much smaller than unity. Therefore, there is no $\log R - \log L_{\rm Ext}$ relationship when R is small and there is an anti-correlation of $\log R - \log L_{\rm Ext}$ when R is large. This correlation implies that a smaller extended luminosity source has a larger core-dominance parameter, R. So, this source shows either large f or large δ since $R \propto f\delta^p$ (Ghisellini et al. 1993).

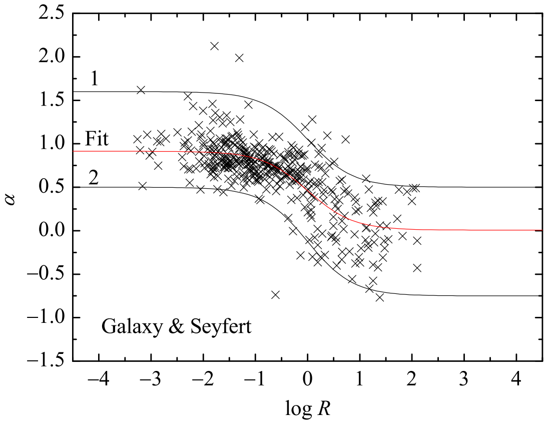

Fig. 7 Plot of the radio spectral index, $\alpha_{\rm t}$, against the core-dominance parameter for galaxies (including Seyfert galaxies). Curve 1 corresponds to $\alpha_{\rm C}$ (or $\alpha_{\rm j}$) = 0.5 and $\alpha_{\rm Ext}$ (or $\alpha_{\rm unb}$) = 1.60, curve 2 corresponds to $\alpha_{\rm C} = -0.75$ and $\alpha_{\rm Ext} = 0.5$, and the fitting curve corresponds to $\alpha_{\rm C} = -0.01$ and $\alpha_{\rm Ext} = 0.91$.

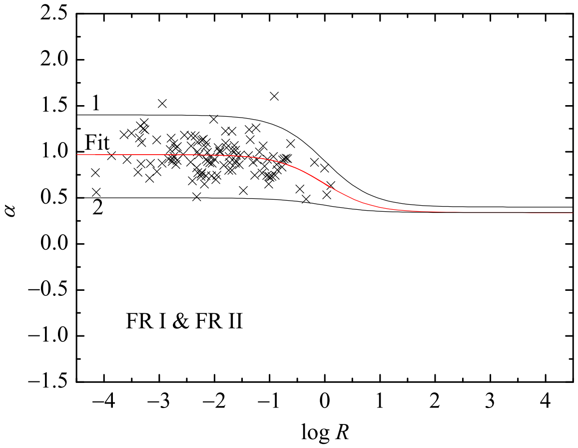

Fig. 8 Plot of the radio spectral index, $\alpha_{\rm t}$, against the core-dominance parameter for FRI/II galaxies. Curve 1 corresponds to $\alpha_{\rm C}$ (or $\alpha_{\rm j}$) = 0.4 and $\alpha_{\rm Ext}$ (or $\alpha_{\rm unb}$) = 1.40, curve 2 corresponds to $\alpha_{\rm C}$ = 0.34 and $\alpha_{\rm Ext} = 0.5$, and the fitting curve corresponds to $\alpha_{\rm C}$= 0.34 and $\alpha_{\rm Ext} = 0.97$.

This correlation is perhaps from an evolutionary result. If "young" AGNs have a strong beamed component indicating strong ongoing activity, but the extended emission has not yet had time to accumulate, then the "young" sources have weak extended emission and strong beamed emission, resulting in large $\log R$.

When we considered the relationship between the core-dominance parameter ($\log R$) and redshift ($\log z$), we have $\log R = (0.48 \pm 0.06) \log z - 0.15 \pm 0.04$, with a correlation coefficient of $r = 0.24$; the result is shown in Figure 9. It shows an approximate evolutionary effect.

However, this kind of correlation is probably from some selection effects. If both $L_{\rm Ext}$ and $L_{\rm C}$ have a distribution with upper and lower limits, then one is more likely to find a larger R for a source with $L_{\rm Ext}$ close to the lower luminosity limit, and vice versa. Also, it is possible that the source

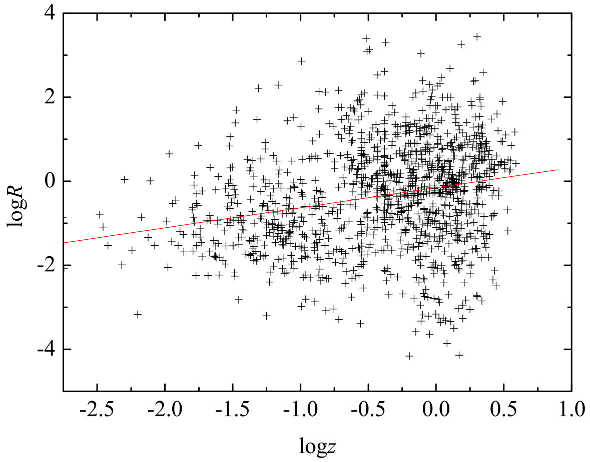

Fig. 9 Plot of the core-dominance parameter against redshift.

Table 7 Linear Regression Results for Core-luminosity, Extended Luminosity and Redshift ($N = 1223$, $p < 10^{-4}$)

	$(a \pm \Delta a)$	$(b \pm \Delta b)$	Corr. Coef.
$\log L_{\rm E} - \log L_{\rm C}$	0.98 ± 0.02	0.28± 0.62	0.76
$\log z - \log L_{\rm C}$	2.69 ± 0.04	26.69± 0.03	0.87
$\log z - \log L_{\rm E}$	2.09 ± 0.03	26.67± 0.03	0.76
$\log z - \log R$	0.48 ± 0.06	−0.15± 0.04	0.24

with larger δ is brighter, and it can be detected much more easily, therefore, we can get an apparent anti-correlation between the core-dominance parameter and the extended luminosity.

For the core-luminosity and the extended-luminosity, we found that they are correlated with a correlation coefficient of $r_{\rm C-E} = 0.76$ and a chance probability of $p < 10^{-4}$ (see Table 7); $\log L_{\rm C} = (0.98 \pm 0.02) \log L_{\rm Ext} + 0.28 \pm 0.62$, and the corresponding figure is shown in Figure 10.

When the redshift dependence of luminosity is excluded, we found that the correlation coefficient $r_{({\rm C-E})_z} = \frac{r_{\rm C-E} - r_{{\rm C}-z} r_{{\rm E}-z}}{\sqrt{(1-r^2_{{\rm C}-z})(1-r^2_{{\rm E}-z})}}$; here $r_{({\rm C-E})_z}$ is the correlation coefficient between core-luminosity and extended luminosity with the redshift dependence excluded, $r_{({\rm C}-z)}$ is the correlation coefficient between core-luminosity and redshift, and $r_{({\rm E}-z)}$ is the correlation coefficient between extended-luminosity and redshift. From the whole sample, we have $r_{({\rm C}-z)}$ = 0.87 and $r_{({\rm E}-z)}$ = 0.86, so we have $r_{({\rm C-E})_z}$ = 0.1. There is no more correlation between core luminosity and extended luminosity.

It is argued that the parent population of BL Lac objects is FRI galaxies but that of quasars is FRII. Now, we investigate the relationship using the correlation between the extended luminosity and the core-dominance parameter. Since the radio galaxies have a large viewing angle, their beaming effect is very weak, and their log R is very small. In this case, the beamed sources and their parent population should follow the same correlation.

For the BL Lac objects and FRI radio galaxies, we have $\log L_e = -(0.20 \pm 0.09) \log R + (24.78 \pm 0.13)$, with a correlation coefficient of $r = -0.30$ and a chance probability of $p = 3.09 \times 10^{-3}$. The result is shown in Figure 11.

For the quasars and FRII radio galaxies, we have $\log L_e = -(0.21 \pm 0.02) \log R + (26.78 \pm 0.03)$, with a correlation coefficient of $r = -0.32$ and a chance probability of $p < 10^{-4}$. The result is shown in Figure 12.

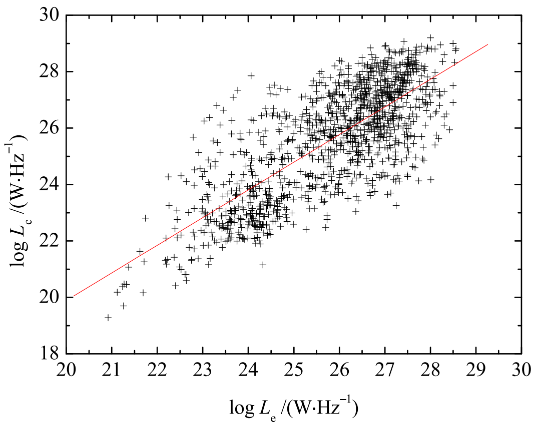

Fig. 10 Plot of the core-luminosity against extended luminosity.

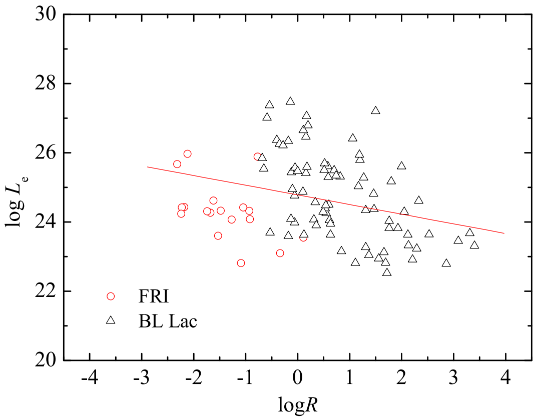

Fig. 11 Plot of the extended luminosity against the core-dominance parameter for BL Lac objects and FRI galaxies. Here triangles (△) stand for BL Lac objects and open circles (○) for FRI galaxies.

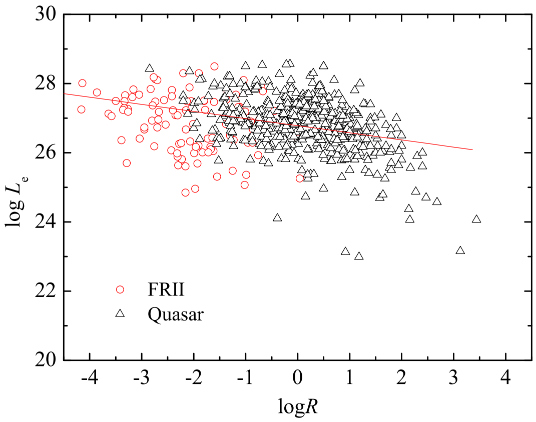

Fig. 12 Plot of the extended luminosity against the core-dominance parameter for quasars and FRII galaxies. Here triangles (△) stand for quasars and open circles (○) for FRII galaxies.

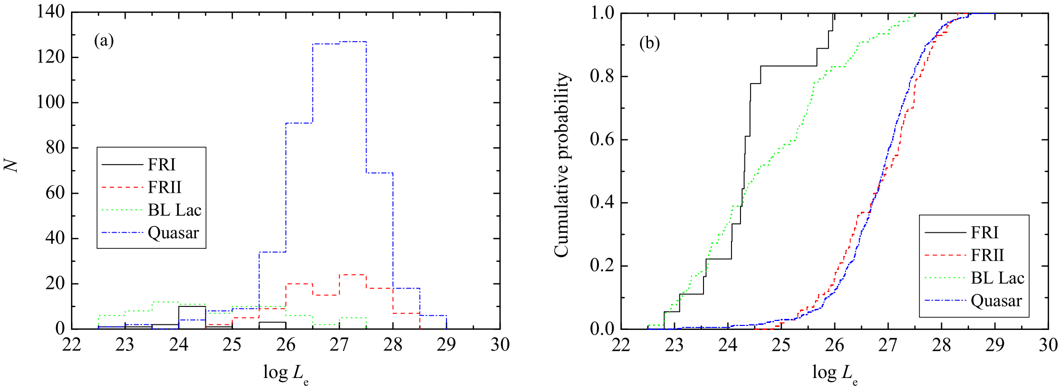

Fig. 13 Distribution of the extended luminosity, (a) and the cumulative probability (b) for FRI (*solid line*), FRII (*broken line*), BL Lac objects (*dotted line*) and quasars (*broken-dotted line*).

In addition, if the population arguments are correct, then one can expect that the distributions of the extended luminosity for a blazar sample should be from the same parent distribution. Therefore, we applied a K-S test to the distributions of blazars and their radio galaxies. We found that the probability for BL Lac objects and the FRI radio galaxies to be from one single distribution is 9%, while the probability for quasars and FRII galaxies is 20% (see Fig. 13). In this sense, we can say that quasars and FRII galaxies should be unified, while BL Lacs and FRI radio galaxies should also be unified.

3.1 Conclusions

In the present work, we compiled the core/extended emissions and total emissions for a sample of 1223 radio sources, calculated the core-dominance parameters and the spectral indexes, investigated the correlation between the radio spectral index and the core dominance parameter, and the correlation between core-dominance parameter and the extended luminosity. From our analysis, we can come to the following conclusions:

(1) The spectral index is dependent on the core dominance parameter, which may be from the relativistic beaming effect.
(2) There is a tendency for the extended luminosity to decrease with the core-dominance parameter.
(3) Quasars should be unified with FRII radio galaxies, and BL Lac objects should be unified with FRI radio galaxies.
(4) For the radio source, α_{C} = 0.07 and α_{Ext} = 0.92 can be adopted.

Acknowledgements The work is partially supported by the National Natural Science Foundation of China (NSFC, Grant Nos. 10633010, 11173009), the National Basic Research Program (973 program, 2007CB815405) and the Bureau of Education of Guangzhou Municipality (No.11 Sui-Jiao-Ke[2009]), Guangdong Province Universities and Colleges Pearl River Scholar Funded Scheme (GDUPS)(2009), Yangcheng Scholar Funded Scheme (10A027S) and the Joint Laboratory for Optical Astronomy of Chinese Academy of Sciences.

References

Abdo, A. A., Ackermann, M., Ajello, M., et al. 2010, ApJ, 715, 429

Aller, M. F., Aller, H. D., & Hughes, P. A. 2003, ApJ, 586, 33

Andruchow, I., Romero, G. E., & Cellone, S. A. 2005, A&A, 442, 97

Antonucci, R. R. J., & Ulvestad, J. S. 1985, ApJ, 294, 158

Barthel, P. D., Vestergaard, M., & Lonsdale, C. J. 2000, A&A, 354, 7

Best, P. N., Carilli, C. L., Garrington, S. T., Longair, M. S., & Rottgering, H. J. A. 1998, MNRAS, 299, 357

Best, P. N., Eales, S. A., Longair, M. S., Rawlings, S., & Rottgering, H. J. A. 1999, MNRAS, 303, 616

Best, P. N., Longair, M. S., & Roettgering, J. H. A. 1997, MNRAS, 292, 758

Biermann, P., Duerbeck, H., Eckart, A., et al. 1981, ApJ, 247, L53

Britzen, S., Brinkmann, W., Campbell, R. M., et al. 2007, A&A, 476, 759

Browne, I. W. A. 1989, in BL Lac Objects, Lecture Notes in Physics, 334, eds. L. Maraschi, T. Maccacaro, & M.-H. Ulrich (Berlin: Springer Verlag), 401

Browne, I. W. A., & Murphy, D. W. 1987, MNRAS, 226, 601

Browne, I. W. A., & Perley, R. A. 1986, MNRAS, 222, 149

Cellone, S. A., Romero, G. E., & Araudo, A. T. 2007, MNRAS, 374, 357

Ciprini, S., Takalo, L. O., Tosti, G., et al. 2007, A&A, 467, 465

Cotton, W. D., Feretti, L., Giovannini, G., Lara, L., & Venturi, T. 1999, ApJ, 519, 108

Dai, B. Z., Li, X. H., Liu, Z. M., et al. 2009, MNRAS, 392, 1181

Efimov, Y. S., Shakhovskoy, N. M., Takalo, L. O., & Sillanpää, A. 2002, A&A, 381, 408

Fan, J.-H. 2002, PASJ, 54, L55

Fan, J. H. 2003, ApJ, 585, L23

Fan, J.-H. 2005, Chinese Journal of Astronomy and Astrophysics Supplement, 5, 213

Fan, J. H., Cheng, K. S., Zhang, L., & Liu, C. H. 1997, A&A, 327, 947

Fan, J.-H., Hua, T.-X., Yuan, Y.-H., et al. 2006, PASJ, 58, 945

Fan, J.-H., Huang, Y., He, T.-M., et al. 2009, PASJ, 61, 639

Fan, J. H., Xie, G. Z., & Bacon, R. 1999, A&AS, 136, 13

Fan, J.-H., Yang, J.-H., Tao, J., Huang, Y., & Liu, Y. 2010, PASJ, 62, 211

Fan, J.-H., Yuan, Y.-H., Liu, Y., et al. 2008, PASJ, 60, 707

Fan, J. H., & Zhang, J. S. 2003, A&A, 407, 899

Feigelson, E. D., Isobe, T., & Kembhavi, A. 1984, AJ, 89, 1464

Garrington, S. T., Conway, R. G., & Leahy, J. P. 1991, MNRAS, 250, 171

Ghisellini, G., Padovani, P., Celotti, A., & Maraschi, L. 1993, ApJ, 407, 65

Gower, A. C., & Hutchings, J. B. 1984, AJ, 89, 1658

Gupta, A. C., Banerjee, D. P. K., Ashok, N. M., & Joshi, U. C. 2004, A&A, 422, 505

Hardcastle, M. J., Alexander, P., Pooley, G. G., & Riley, J. M. 1997, MNRAS, 288, 859

Hintzen, P., & Owen, F. 1981, AJ, 86, 1577

Hintzen, P., Ulvestad, J., & Owen, F. 1983, AJ, 88, 709

Hough, D. H., & Readhead, A. C. S. 1989, AJ, 98, 1208

Hutchings, J. B., Price, R., & Gower, A. C. 1988, ApJ, 329, 122

Kapahi, V. K., Athreya, R. M., Subrahmanya, C. R., et al. 1998, ApJS, 118, 327

Kollgaard, R. I., Wardle, J. F. C., & Roberts, D. H. 1990, AJ, 100, 1057

Kovalev, Y. Y., Kellermann, K. I., Lister, M. L., et al. 2005, AJ, 130, 2473

Kurtanidze, O. M., Nikolashvili, M. G., Kimeridze, G. N., Sigua, L. A., & Kapanadze, B. Z. 2007, in IAU Symposium 238, eds. V. Karas, & G. Matt, 399

Lähteenmäki, A., & Valtaoja, E. 1999, ApJ, 521, 493

Landt, H., Perlman, E. S., & Padovani, P. 2006, ApJ, 637, 183

Leahy, J. P., & Perley, R. A. 1991, AJ, 102, 537

Liu, F. K., & Zhang, Y. H. 2002, A&A, 381, 757
Ludke, E., Garrington, S. T., Spencer, R. E., et al. 1998, MNRAS, 299, 467
Maraschi, L., & Rovetti, F. 1994, ApJ, 436, 79
Miley, G. K., & Hartsuijker, A. P. 1978, A&AS, 34, 129
Murphy, D. W., Browne, I. W. A., & Perley, R. A. 1993, MNRAS, 264, 298
Neff, S. G., & Hutchings, J. B. 1990, AJ, 100, 1441
Neff, S. G., Hutchings, J. B., & Gower, A. C. 1989, AJ, 97, 1291
Neff, S. G., Roberts, L., & Hutchings, J. B. 1995, ApJS, 99, 349
O'Dea, C. P., & Owen, F. N. 1985a, AJ, 90, 954
O'Dea, C. P., & Owen, F. N. 1985b, AJ, 90, 927
Orr, M. J. L., & Browne, I. W. A. 1982, MNRAS, 200, 1067
Owen, F. N., Porcas, R. W., & Neff, S. G. 1978, AJ, 83, 1009
Padovani, P., & Urry, C. M. 1992, ApJ, 387, 449
Parma, P., de Ruiter, H. R., & Cameron, R. A. 1991, AJ, 102, 1960
Pedro, R. C., & Priyamvada, N. 2007, NJPh, 9, 445
Perley, R. A. 1982, AJ, 87, 859
Perley, R. A., Fomalont, E. B., & Johnston, K. J. 1982, ApJ, 255, L93
Perlman, E. S., & Stocke, J. T. 1993, ApJ, 406, 430
Potash, R. I., & Wardle, J. F. C. 1979, AJ, 84, 707
Price, R., Gower, A. C., Hutchings, J. B., Talon, S., Duncan, D., & Ross, G. 1993, ApJS, 86, 365
Punsly, B. 1995, AJ, 109, 1555
Qin, Y.-P., Xie, G.-Z., Bai, J.-M., et al. 1998, A&A, 333, 790
Readhead, A. C. S. 1994, ApJ, 426, 51
Riley, J. M., Rawlings, S., McMahon, R. G., et al. 1999, MNRAS, 307, 293
Romero, G. E., Cellone, S. A., Combi, J. A., & Andruchow, I. 2002, A&A, 390, 431
Romero, G. E., Chajet, L., Abraham, Z., & Fan, J. H. 2000, A&A, 360, 57
Saikia, D. J., Holmes, G. F., Kulkarni, A. R., Salter, C. J., & Garrington, S. T. 1998, MNRAS, 298, 877
Saikia, D. J., Junor, W., Cornwell, T. J., Muxlow, T. W. B., & Shastri, P. 1990, MNRAS, 245, 408
Saikia, D. J., Salter, C. J., Neff, S. G., et al. 1987a, MNRAS, 228, 203
Saikia, D. J., Shastri, P., Cornwell, T. J., Junor, W., & Muxlow, T. W. B. 1989, Journal of Astrophysics and Astronomy, 10, 203
Saikia, D. J., Wiita, P. J., & Cornwell, T. J. 1987b, MNRAS, 224, 53
Scheuer, P. A. G., & Readhead, A. C. S. 1979, Nature, 277, 182
Schoenmakers, A. P., de Bruyn, A. G., Röttgering, H. J. A., & van der Laan, H. 2000, MNRAS, 315, 395
Spencer, R. E., Schilizzi, R. T., Fanti, C., et al. 1991, MNRAS, 250, 225
Taylor, G. B., Vermeulen, R. C., Readhead, A. C. S., et al. 1996, ApJS, 107, 37
Ulrich, M. H. 1989, in BL Lac Objects, Lecture Notes in Physics, 334, eds. L. Maraschi, T. Maccacaro, & M.-H. Ulrich (Berlin: Springer Verlag), 45
Ulvestad, J. S., & Antonucci, R. R. J. 1986, AJ, 92, 6
Urry, C. M., & Padovani, P. 1995, PASP, 107, 803
Wagner, S. J. 1996, A&AS, 120, C495
Wills, B. J., & Browne, I. W. A. 1986, ApJ, 302, 56
Wills, B. J., Wills, D., Breger, M., Antonucci, R. R. J., & Barvainis, R. 1992, ApJ, 398, 454
Wrobel, J. M., Harrison, B., Pedlar, A., & Unger, S. W. 1988, MNRAS, 235, 663
Wu, J., Zhou, X., Peng, B., et al. 2005, MNRAS, 361, 155
Xie, G. Z., Liu, H. T., Cha, G. W., et al. 2005, AJ, 130, 2506
Xie, G. Z., Zhang, Y. H., Fan, J. H., & Liu, F. K. 1993, A&A, 278, 6
Xie, G. Z., Zhou, S. B., Dai, B. Z., et al. 2002, MNRAS, 329, 689
Zhang, Y.-W., & Fan, J.-H. 2008, ChJAA (Chin. J. Astron. Astrophys.), 8, 385